International Journal of Electrical, Electronic and Communication Sciences
ISSN: 2517-9438
Vol:14, No:9, 2020

Implementation of Channel Estimation and Timing Synchronization Algorithms for MIMO-OFDM System Using NI USRP 2920

Ali Beydoun, Hamzé H. Alaeddine

Abstract—MIMO-OFDM communication system presents a key solution for the next generation of mobile communication due to its high spectral efficiency, high data rate and robustness against multi-path fading channels. However, MIMO-OFDM system requires a perfect knowledge of the channel state information and a good synchronization between the transmitter and the receiver to achieve the expected performances. Recently, we have proposed two algorithms for channel estimation and timing synchronization with good performances and very low implementation complexity compared to those proposed in the literature. In order to validate and evaluate the efficiency of these algorithms in real environments, this paper presents in detail the implementation of 2×2 MIMO-OFDM system based on LabVIEW and USRP 2920. Implementation results show a good agreement with the simulation results under different configuration parameters.

Keywords—MIMO-OFDM system, timing synchronization, channel estimation, STBC, USRP 2920.

I. Introduction

WIRELESS mobile communication has seen exponential increase in the data rate in the last few years as a result of integrating new data intensive applications such as high-definition video streaming, smart health monitoring and Internet of Things (IoT) [1]- [3]. Since the spectrum is a scarce resource, the combination of Multiple Input Multiple-Output (MIMO) system with Orthogonal Frequency Division Multiplexing (OFDM) modulation technique presents a key solution to achieve high data rates as well as high quality of service. Indeed, OFDM has attracted a lot of attention to achieve higher data rate over wireless channel thanks to its higher spectral efficiency, its simplicity and its robustness against frequency selective channels by dividing the entire channel into many narrow flat fading orthogonal sub-channels which reduces the Inter-Carrier Interference and the Inter-Symbol Interference (ISI) [4]. Moreover, MIMO system using multiple antennas at the both sides of the transceiver [5], allows to increase the link capacity by sending different data stream over different transmit antenna or to improve the link reliability by sending the same data stream over different antenna using Space Time Block Code (STBC) [6]. However, MIMO-OFDM system faces two main challenges to maintain the expected theoretical performances:

- First, the timing synchronization between the transmitter and the receiver. In fact, incorrect timing synchronization introduces inter-carrier interference and leads to apply the FFT at the receiver side at the undesired position which prevents the OFDM signal to be correctly decoded. Several timing synchronization approaches have been proposed for MIMO-OFDM system in the literature based on the Schmidl and Cox algorithm [7]- [10]. These algorithms have high computational complexity and high execution time as they perform the synchronization in two steps. To overcome these problems, a new algorithm was proposed in [11]. The proposed algorithm achieves the synchronization in one step using CAZAC sequence inserted in the time domain in order to not involve the FFT in the synchronization process and to reduce consequently the execution time.
- Secondly, the estimation of the Channel State Information (CSI) at the receiver side in order to recover the transmitted data correctly. Several approaches for channel estimation have been proposed in the literature using either least square (LS) or minimum mean squared error (MMSE) estimators. These algorithms suffer from high computational complexity as they require the inversion of large matrices. In order to reduce the channel estimation complexity, a new algorithm was proposed in [12] that takes advantage of the use of the STBC encoder to transform the estimation process into a simple linear operation and consequently reduces considerably the computational complexity.

As previously highlighted, the aim of this paper is to implement a 2×2 MIMO-OFDM system using USRP 2920 in order to validate the efficiency of the proposed algorithms in real environments.

The remaining of this paper is organized as follows: Section II introduces the MIMO-OFDM system model. The proposed timing synchronization and channel estimation algorithms are briefly described in Section III. Section IV describes in detail the LabVIEW implementation design of the MIMO-OFDM transceiver. Finally, Section V is dedicated for conclusion.

II. MIMO-OFDM System Model

A 2×2 MIMO-OFDM system with two transmit antennas and two receive antennas using the STBC-Alamouti encoder is shown in Fig.1. The binary data to be transmitted are first mapped to the complex modulation symbols by using M-QAM signal constellation. The QAM symbols are then multiplexed with pilot symbols used in the channel estimation (see Section

Ali Beydoun and Hamzé H. Alaeddine are with the Department of Physics, Lebanese University, Beirut, Lebanon (e-mail: ali.beydoun@ul.edu.lb, hamze.alaeddine@ul.edu.lb).

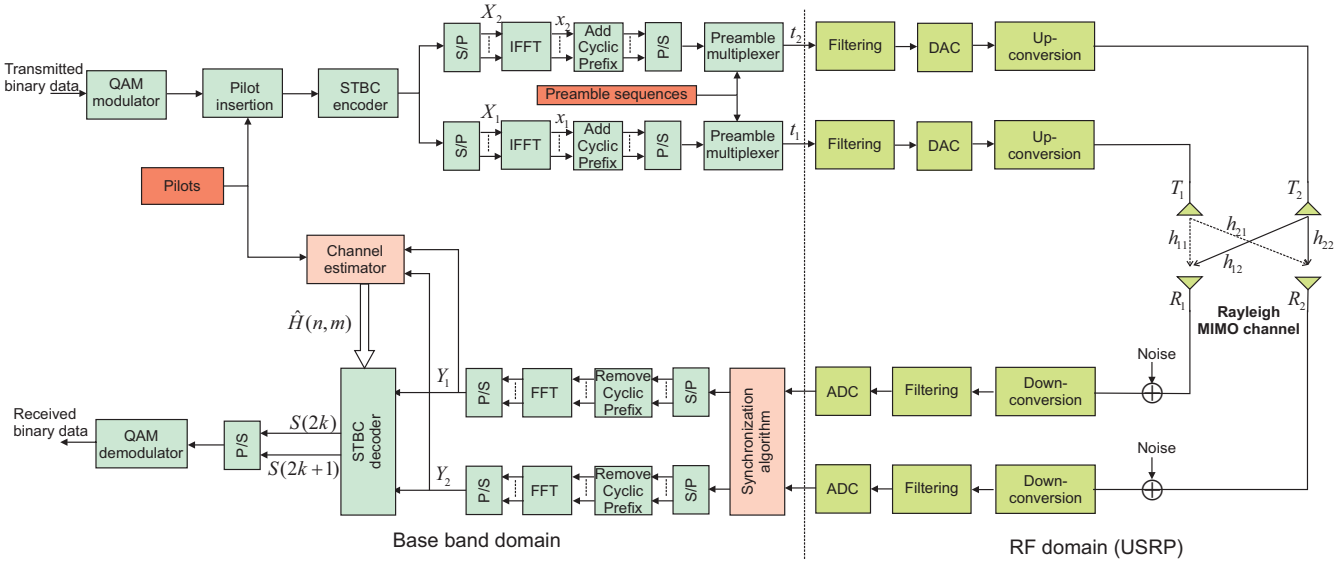

Fig. 1 Simplified block diagram of MIMO-OFDM system

III). Afterwards, the resulting symbols are fed to the STBC encoder (Space-Time Block Coding) to exploit the spatial diversity and to increase the reliability of transmission with the codeword matrix illustrated in Table I [13].

TABLE I
ENCODED DATA ACCORDING TO TIME AND SUBCARRIER

Subcarrier index	Antenna 1	Antenna 2
Even index $(2k)$	$S_1[2k]$	$S_2[2k]$
Odd index $(2k+1)$	$S_1[2k+1] = -S_2^*[2k]$	$S_2[2k+1] = S_1^*[2k]$

Then, the encoder outputs pass through a serial to parallel converters to generate two frames X_1 and X_2 of N samples at the input of the IFFT blocks:

$$\mathrm{X}_1 = (S[0] - S^*[1]\ S[2] - S^*[3] \cdots\cdots - S^*[N-1]) \quad (1)$$

$$\mathrm{X}_2 = (S[1]\ S^*[0]\ S[3]\ S^*[2] \cdots\cdots S^*[N-2]) \quad (2)$$

Next, the Inverse Fast Fourier Transform (IFFT) is applied to generate the OFDM symbols x_1 and x_2 in the time domain. A cyclic prefix (CP), the replica of last part of the OFDM symbol, is attached at the beginning of each time domain OFDM symbol to preserve the orthogonality between subcarriers and to eliminate interference between the adjacent OFDM symbols. The length of CP must exceed the maximum excess delay of the multipath propagation channel [4]. After the insertion of CP, the resultant OFDM symbols are first converted to serial form and then multiplexed with preamble sequences for the timing synchronization before being transmitted simultaneously over the 2×2 AWGN Rayleigh channel. The OFDM symbol transmitted from the j^{th} antenna is given by [4]:

$$x_j(n) = \frac{1}{\sqrt{N}} \sum_{k=0}^{N-1} X_j(k) e^{j\frac{2\pi nk}{N}} \quad (3)$$

where $X_j(k)$ is the transmitted symbol in the frequency domain before the IFFT and N is the number of sub-carriers for one OFDM symbol. The signal is then filtered and up-converted to the RF domain using the RF hardware interface provided by the USRP. The Rayleigh channel between i^{th} receive antenna and j^{th} transmit antenna is given by:

$$h_{ij}(t) = \sum_{l=0}^{L-1} \alpha_{ij}^l \delta\left(t - \tau_{ij}^l\right) \quad (4)$$

where L is the number of multi-path channels between i^{th} receiver and j^{th} transmitter. α_{ij}^l denotes the channel gain and τ_{ij}^l denotes the delay of the path. The received signal r_i, on each receive antenna R_i, is the convolution of the channel impulse response and the transmitted signal and is given by:

$$r_i(t) = \sum_{j=1}^{2} \sum_{l=0}^{L} \left(\alpha_{ij}^l \delta\left(t - \tau_{ij}^l\right) * t_j(t)\right) + n_i(t),\ i = 1, 2 \quad (5)$$

where t_j is the transmitted signal on the transmit antenna T_j, n_i is the additive white Gaussian noise (AWGN).

At the receiver side, the received signal is down-converted first to the baseband. Then, the timing synchronization algorithm is applied to detect the beginning of the OFDM symbols and ensure correct demodulation. After a good timing synchronization, the cyclic prefix of each OFDM symbol is removed. Then, the signal returns back into frequency domain thanks to the FFT block. It is important to note that, if the cyclic prefix length is higher than or equal the number of multipaths (L) of the 2×2 AWGN Rayleigh channel, the linear convolution of the transmitted signal with the channel impulse response is converted into circular convolution and therefore the FFT output can be expressed as:

$$Y_i(k) = \sum_{j=1}^{N_t=2} X_j(k) H_{ij}(k) + N_i(k) \quad i = 1, 2 \quad (6)$$

where Y_i is the received OFDM symbol, X_j the transmitted OFDM symbol, H_{ij} is the frequency response of the channel

between i^{th} receive antenna and j^{th} transmit antenna on the k^{th} subcarrier of the OFDM symbol, and N_i is the additive complex Gaussian noise with zero mean and variance σ_N^2.

The FFT outputs are first converted into serial and then sent to the STBC decoder that estimates the transmitted OFDM symbols using the channel state information delivered by the channel estimator.

Based on the assumption, that the channel frequency response remains approximately constant over two adjacent (odd and even) subcarriers [12]:

$$\hat{H}_{ij}(2k) = \hat{H}_{ij}(2k+1) \tag{7}$$

the estimated even and odd symbols by the STBC decoder are given by [12]:

$$\tilde{S}(2k) = \frac{\sum_{i=1}^{2} \hat{H}_{i1}^{*}(2k)\, Y_i(2k) + \hat{H}_{i2}(2k)\, Y_i^{*}(2k+1)}{\sum_{i=1}^{2}\sum_{j=1}^{2} \left\|\hat{H}_{ij}(2k)\right\|^2} \tag{8}$$

$$\tilde{S}(2k+1) = \frac{\sum_{i=1}^{2} \hat{H}_{i2}^{*}(2k)\, Y_i(2k) - \hat{H}_{i1}(2k)\, Y_i^{*}(2k+1)}{\sum_{i=1}^{2}\sum_{j=1}^{2} \left\|\hat{H}_{ij}(2k)\right\|^2} \tag{9}$$

After that, a Maximum Likelihood detector is used to associate the estimated values to the nearest symbols in the QAM constellation. Finally, a QAM demodulator is used to demodulate and recover the binary data.

III. Review of the Proposed Algorithms

A. Timing Synchronization Algorithm

In order to reduce the execution time and the complexity, the timing synchronization algorithm proposed in [11] performs the synchronization in single step. It is based on sending a synchronization preamble in the time domain after the OFDM modulator (see Fig. 1). The main characteristic of the synchronization preamble is to have good autocorrelation and cross-correlation properties in order to detect a correlation peak as closed as possible to a Dirac pulse. On the other hand, the synchronization preambles should be orthogonal to eliminate the interferences between preambles at simultaneous transmissions in MIMO system. The preamble used in this algorithm is simply the CAZAC sequence given by:

$$C(k) = \begin{cases} e^{j\frac{\pi M k(k+1)}{L_c}} & if\ \ L_c\ \ is\ odd \\ e^{j\frac{\pi M k^2}{L_c}} & if\ \ L_c\ \ is\ even \end{cases} \tag{10}$$

where L_C is the length of CAZAC sequence, M is a natural number relatively prime to L_C and $0 \leq k \leq L_c - 1$. It is important to note that the prime number M must be carefully chosen from the set of prime numbers $\mathbb{M}$. Indeed, not all prime numbers give the same auto-correlation function [11].

At the receiver side, the proposed synchronization algorithm correlates simultaneously the received signal on each antenna R_j with the known sequences P_1 and P_2 as shown in Fig. 2.

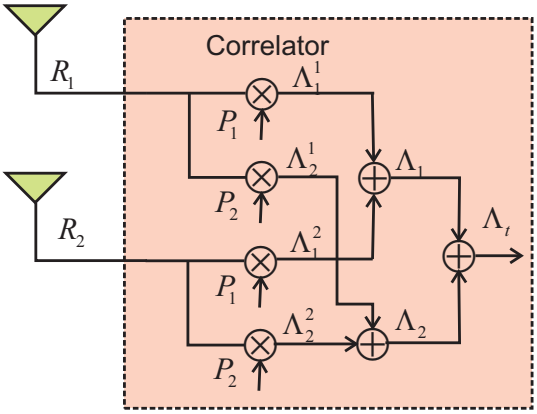

Fig. 2 Synchronization module.

Afterwards, the timing synchronization estimate is chosen as the argument that maximizes the squared modulus of the timing metric function $\|\lambda(d)\|^2$ and is denoted by $\hat{\tau}$:

$$\hat{\tau} = \arg \max_{d} \left(\|\lambda(d)\|^2 \right) \tag{11}$$

Three expressions could be considered for the timing metric function $\lambda(d)$:

1)

$$\lambda(d) = \Lambda_i^j(d) = r_j \otimes P_i = \sum_{m=0}^{L_p-1} r_j(d+m) P_i^*(m) \tag{12}$$

where i and $j \in [1,2]$ and $\otimes$ denotes the correlation operation. In this case, one correlator is needed and the timing metric $\lambda(d)$ is simply the correlation between any received signal r_j with any preamble sequence P_i.

2)

$$\lambda(d) = \Lambda_i(d) = \sum_{j=1}^{2} \Lambda_i^j(d) \quad i = 1,2 \tag{13}$$

The received signals at both antennas are correlated with the same sequence P_i and added together in order to increase the acquisition probability.

3)

$$\lambda(d) = \Lambda_t(d) = \sum_{i=1}^{2}\sum_{j=1}^{2} \Lambda_i^j(d) \tag{14}$$

To further increase the acquisition probability, the received signals at different antennas are correlated with both preambles and combined together in a way similar to Maximum Ratio Combining (MRC).

B. Channel Estimation Algorithm

The low complex channel estimation algorithm proposed in [12] is based on block type arrangement. It consists to insert pilot symbol between OFDM data symbols in periodic intervals of OFDM blocks. The pilot symbol, which is known at the receiver, is given by :

$$P = [P(0)\ P(1)\ P(2) \cdots P(N-1)] \tag{15}$$

It can be composed of either CAZAC sequences (10) or constant amplitude complex number on all subcarriers. After applying the STBC encoder, the inputs of the IFFT blocks are given by:

$$X_1 = [P(0) - P^*(1) \cdots P(2k) - P^*(2k+1) \cdots - P^*(N-1)] \tag{16}$$

$$X_2 = [P(1)\ P^*(0) \cdots P(2k+1)\ P^*(2k) \cdots P^*(N-2)] \tag{17}$$

As the method is based on STBC, channel parameters have been assumed constant over two adjacent subcarriers (7). Therefore, at the receiver side, the output of the FFT block (6) in the first branch at two adjacent subcarriers can be expressed by the following matrix form:

$$\begin{bmatrix} Y_1(2k) \\ Y_1(2k+1) \end{bmatrix} = \begin{bmatrix} P(2k) & P(2k+1) \\ -P^*(2k+1) & P^*(2k) \end{bmatrix} \begin{bmatrix} H_{11}(2k) \\ H_{12}(2k) \end{bmatrix} + \begin{bmatrix} N_1(2k) \\ N_2(2k+1) \end{bmatrix} \tag{18}$$

Then multiplying both sides of (18) by the matrix:

$$\begin{bmatrix} P^*(2k) & -P(2k+1) \\ P^*(2k+1) & P(2k) \end{bmatrix} \tag{19}$$

The resulting equation is:

$$\begin{bmatrix} P^*(2k) & -P(2k+1) \\ P^*(2k+1) & P(2k) \end{bmatrix} \begin{bmatrix} Y_1(2k) \\ Y_1(2k+1) \end{bmatrix} = \left(\|P(2k)\|^2 + \|P(2k+1)\|^2\right) \begin{bmatrix} H_{11}(2k) \\ H_{12}(2k) \end{bmatrix} + \underbrace{\begin{bmatrix} P^*(2k) & -P(2k+1) \\ P^*(2k+1) & P(2k) \end{bmatrix} \begin{bmatrix} N_1(2k) \\ N_2(2k+1) \end{bmatrix}}_{Noise} \tag{20}$$

The first row of (20) gives:

$$H_{11}(2k) = \frac{P^*(2k)Y_1(2k) - P(2k+1)Y_1(2k+1)}{\|P(2k)\|^2 + \|P(2k+1)\|^2} + \underbrace{\frac{P^*(2k)N_1(2k) - P(2k+1)N_2(2k+1)}{\|P(2k)\|^2 + \|P(2k+1)\|^2}}_{Error} \tag{21}$$

Therefore, the channel parameters can be estimated by:

$$\hat{H}_{11}(2k) = \frac{P^*(2k)Y_1(2k) - P(2k+1)Y_1(2k+1)}{\|P(2k)\|^2 + \|P(2k+1)\|^2} \tag{22}$$

$$\hat{H}_{12}(2k) = \frac{P^*(2k+1)Y_1(2k) + P(2k)Y_1(2k+1)}{\|P(2k)\|^2 + \|P(2k+1)\|^2} \tag{23}$$

In the same way, the other channel parameters can be estimated using the output Y_2 in the second branch:

$$\hat{H}_{21}(2k) = \frac{P^*(2k)Y_2(2k) - P(2k+1)Y_2(2k+1)}{\|P(2k)\|^2 + \|P(2k+1)\|^2} \tag{24}$$

$$\hat{H}_{22}(2k) = \frac{P^*(2k+1)Y_2(2k) + P(2k)Y_2(2k+1)}{\|P(2k)\|^2 + \|P(2k+1)\|^2} \tag{25}$$

It is important to note that due to the orthogonality in the STBC encoder, the channel parameters are estimated using simple linear operation instead of large matrices inversion required in LS and MMSE algorithms. Thus, the implementation complexity is considerably reduced. Moreover, it is clear, from (21) that the estimation error can be reduced significantly by increasing the pilot's amplitude. However, the amplitude of the pilots is limited by the power amplifier in order to stay in the linear operating region and avoid any kind of non linearities that generate interference on the adjacent OFDM bands [14].

IV. Test Bed of 2 × 2 MIMO OFDM System Using NI USRP 2920

A. Hardware Configuration

The 2 × 2 MIMO-OFDM system is implemented on the software defined radio platform USRP 2920 (Universal Software Radio Peripheral) provided by National Instruments. USRP 2920 is mainly composed of an RF amplifier, a local oscillator (LO), an analog to digital converter (ADC), a digital to analog converter (DAC) and two omni-directional antennas. It allows to convert the RF signal to the desired digital baseband signal and vice versa. The USRP 2920 supports frequencies in the range 50 MHz-2.2 GHz with up to 20 MHz bandwidth, which covers the main bandwidths used for mobile communications [15]. Each USRP has a separate transmitter and receiver alloted in a single hardware. As the isolation between the transmitter and the receiver is weak, so four USRP transceivers are used for a 2 × 2 MIMO-OFDM system. The hardware architecture of the system is shown in Fig. 3 and represented pictorially in Fig. 4. The hardware set at each transceiver side consist of two USRPs connected together by MIMO cable to share the clock signal for synchronization purpose. One of the USRPs is connected through one Gigabit Ethernet cable to the host computer where the MIMO-OFDM system is developed using LabVIEW programming environment. The assigned IP addresses shown in Fig. 3 must be in the same subnet as the host computer.

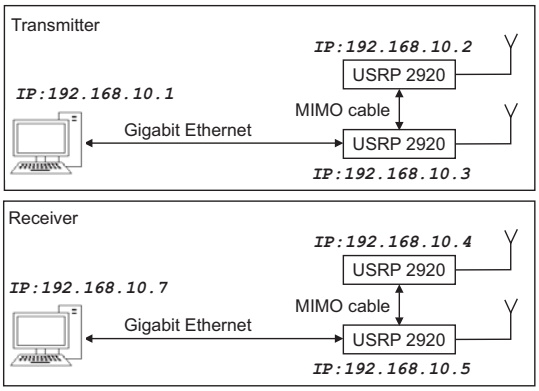

Fig. 3 Structure overview of the testbed

B. LabVIEW Graphical System Design

In our testbed, the MIMO-OFDM system and the hardware control were implemented in LabVIEW on the host computers.

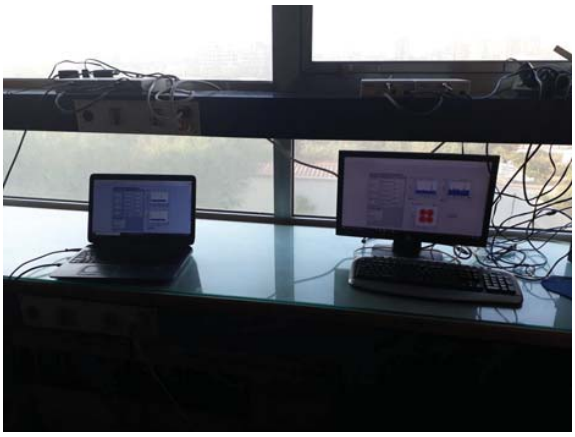

Fig. 4 Hardware setup of 2×2 MIMO-OFDM system platform using NI USRP 2920

LabVIEW is a graphical programming language that includes several communication and signal processing toolkits needed to build our application. Moreover, LabVIEW provides driver functions that interface the host computer with the NI USRP boards [15] that comprise the analog front end and the RF part. The LabVIEW code is composed of two parts: the front panel window which is the graphical user interface and the block diagram window that contains the graphical source code.

1) LabVIEW Front Panels: Figs. 5 and 6 show the LabVIEW front panels at the transmitter and receiver sides. They are mainly composed of two parts. The first part, divided into three tabs, provides information about basic configuration settings. The first tab is reserved for USRPs configuration parameters: IP addresses, IQ rate, carrier frequency, active antenna, antenna gain and the number of samples per fetch in the receiver case only. The second tab concerns the MIMO-OFDM system parameters including the constellation size, the FFT size, the cyclic prefix length, the number of symbols to generate at the transmitter side, the number of transmitters, the number of receivers, the CAZAC sequence length, the type of synchronization preamble [11] and the pilot type for channel estimation [12]. Other parameters like channel length and signal to noise ratio are used only for simulation purposes. Finally, the last tab is reserved to indicate to the user the types and sources of experimental errors that stop the system. On the other hand, the second part provides several plots of the modulus of the transmitted and received signals in the time domain.

2) LabVIEW Block Diagrams : Fig. 7 shows the complete block diagram of the implemented MIMO-OFDM transmitter. Blocks numbered 1 through 5 are used to configure the USRPs using the configuration parameters provided by the user. The other blocks (subVIs) implement the different digital signal processing (DSP) blocks required to generate the two transmitted OFDM signals as previously described in Fig.1. All DSP blocks (blocks numbered 7 through 13) were first written and tested in MATLAB and then ported over to LabVIEW using embedded MATLAB-script blocks. The two channels generated signals t_1 and t_2 are appended to 2D array and then passed, using the subVI *niUSRP Write Tx*, to the USRPs over the Gigabit Ethernet cable. The USRPs upconvert the signals to RF according to the USRPs configuration set up in LabVIEW. Afterward, the USRPs amplify and transmit the signals over the air. As USRPs require a continuous stream of data for transmission or else an underflow occurs at the transmitter, the subVI *niUSRP Write Tx* is enclosed in a while loop so that the same data is repeatedly transmitted.

On the receiver side, the received signals are down-converted by the USRPs from RF using a direct conversion receiver to baseband I/Q components. The digitized I/Q data follows parallel paths through a digital down-conversion process that mixes, filters, and decimates the input signal to a user-specified rate. The down-converted samples are then passed to the host computer over a standard one Gigabit Ethernet connection. An overview of the processing blocks used to implement the receiver is shown in Fig.8. The operations performed in LABVIEW are the reverse process of transmitter section. Blocks numbered 1 through 6 are reserved to configure and synchronize the USRPs in the receiver mode with the configuration parameters provided by the user. It is important to note that the user must configure the transmitter and the receiver with the same parameters in order to demodulate correctly the signal. The other blocks (blocks numbered 7 through 11) implement the different DSP blocks of the 2×2 MIMO-OFDM Receiver (see Fig.1). As already mentioned, all DSP blocks were first written and tested in MATLAB and then ported over to LabVIEW using embedded MATLAB-script blocks. Blocks 9, 10 and 11 are enclosed in a while loop to acquire and demodulate continuously the number of samples requested by the user. The output signal S_w represents the complex data stream at the output of the STBC encoder whereas S represents the ideal complex symbols. Both signals are splitted into real and imaginary in order to plot the constellation graph.

The experiment was conducted using different parameters in indoor environment with carrier frequency of 2 GHz in order to avoid any sources of external interference. The received constellation is shown in Fig.6. From the constellation diagram, it can be shown that the channel and the synchronization algorithms working well and that we have a good agreement between the simulated constellation [12] and the implemented one.

V. Conclusion

In this paper, a 2×2 MIMO-OFDM system platform has been implemented using USRP 2920 as hardware front end device and LabVIEW software in order to test the efficiency of the proposed timing synchronization and channel estimation algorithms [11], [12]. The proposed framework utilizes two USRP 2920 at each side of the transceiver connected by MIMO cable for synchronization purposes. Both baseband signal processing and hardware implementation are detailed. The proposed algorithms were experimented in the testbed at the carrier frequency 2 GHz using different modulation schemes i.e. 4-QAM, 16-QAM and 64-QAM. The constellation graph of the received symbols shows

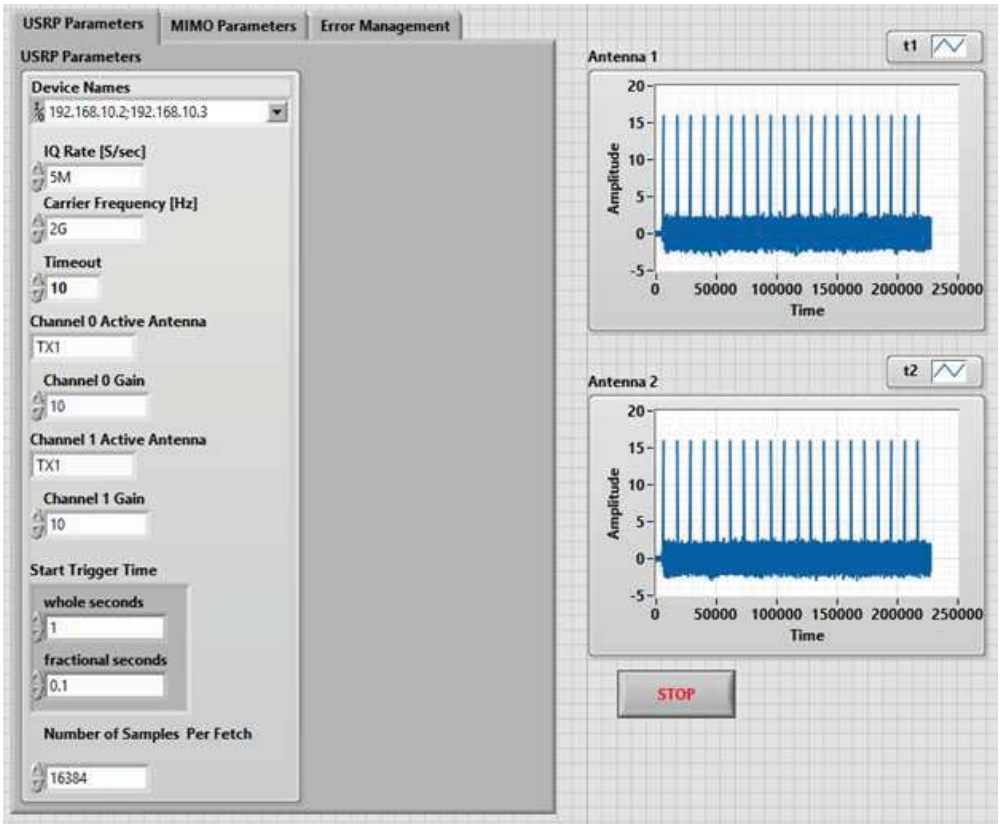

Fig. 5 The LabVIEW front panel of 2 × 2 MIMO-OFDM transmitter including various input configuration parameters in addition to the modulus of transmitted baseband signals on both antennas

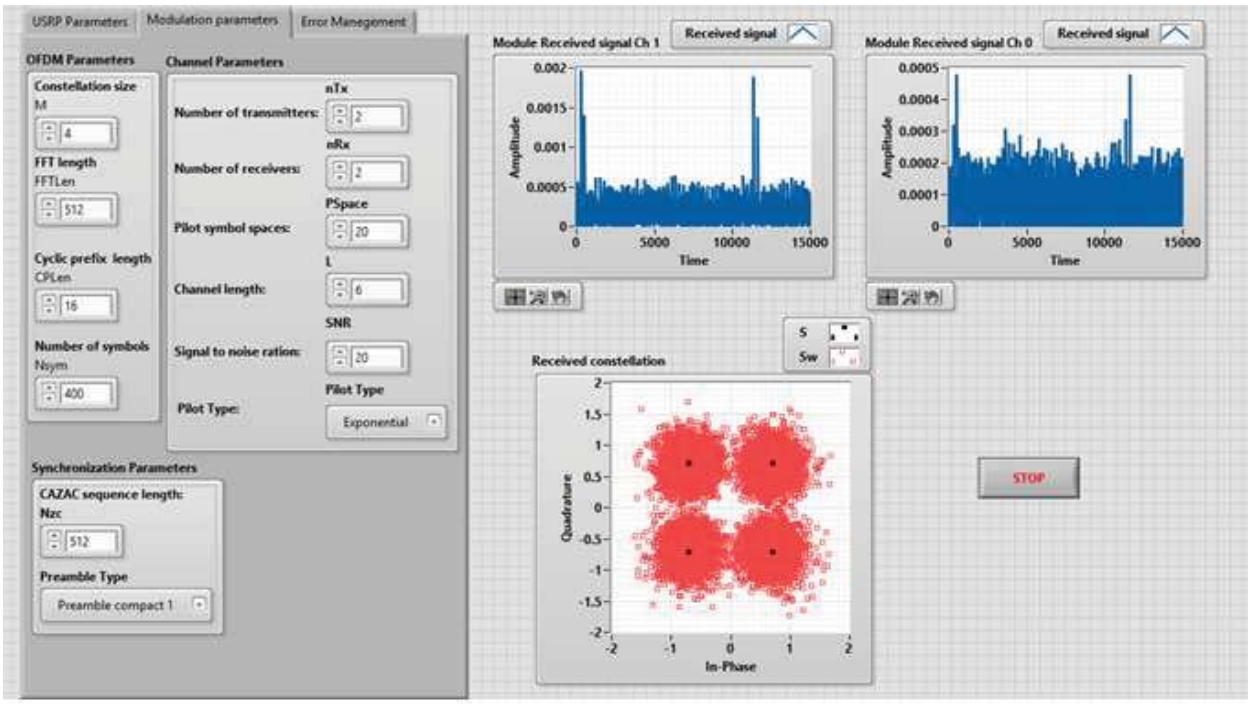

Fig. 6 The LabVIEW front panel of 2 × 2 MIMO-OFDM Receiver including various input configuration parameters, time domain received signals and received symbols constellation graph

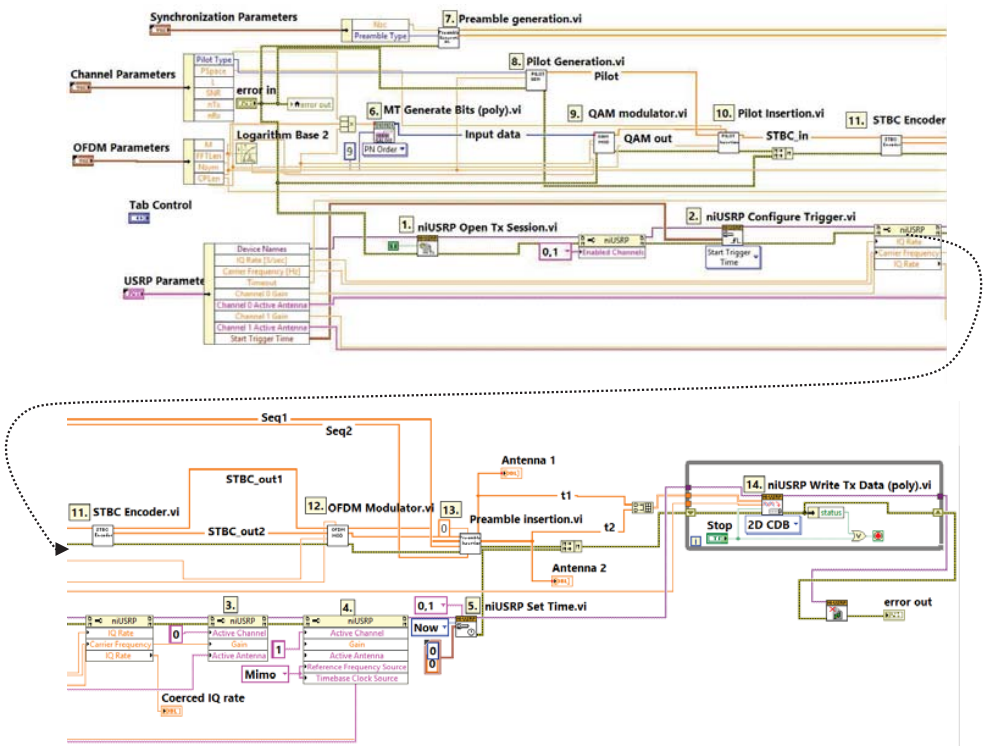

Fig. 7 The LabVIEW block diagram of 2 × 2 MIMO-OFDM Transmitter

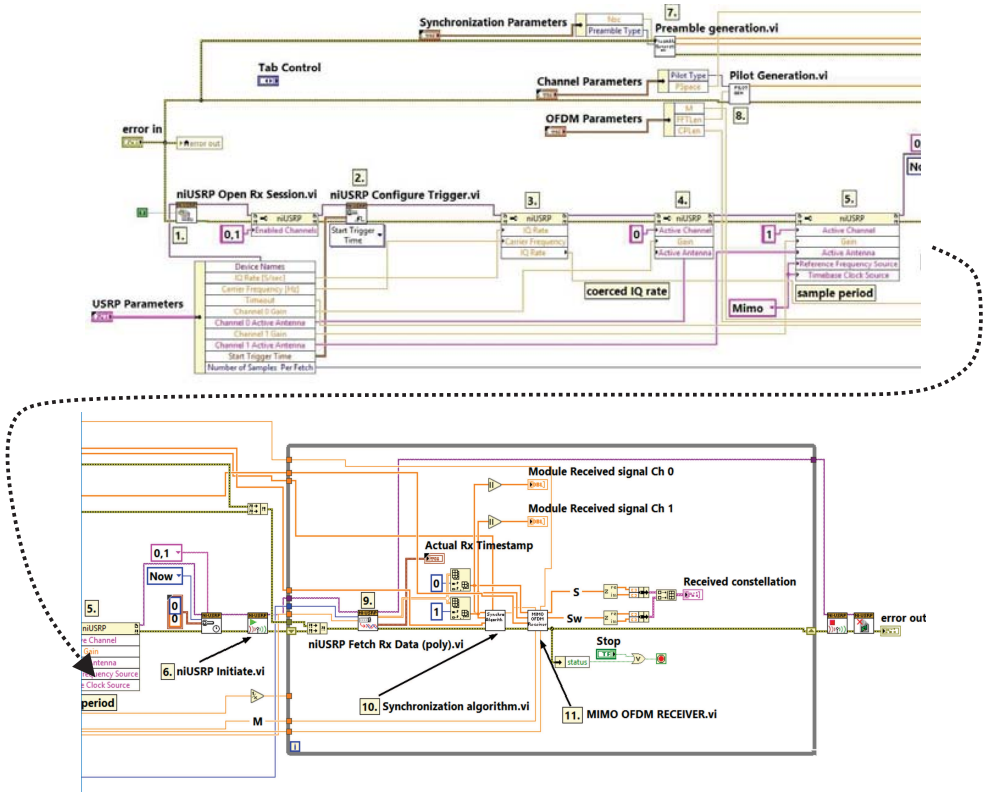

Fig. 8 The LabVIEW block diagram of 2 × 2 MIMO-OFDM Receiver

the efficiency of both algorithms in real environment to recover the transmitted symbols. Moreover, there is a good agreement between the simulated and the experimented system performance. Finally, It is important to mention that the proposed algorithms could be extended without any loss of generality to higher order MIMO systems. These tasks would be our future works.

Acknowledgment

This work is supported by the Lebanese University research program.

References

[1] Y. Zhuang, J. Cappos, T. S. Rappaport, and R. McGeer, "Future Internet bandwidth trends: An investigation on current and future disruptive technologies", *Secure Systems Lab, Dept. Comput. Sci. Eng., Polytech. Inst.* New York Univ., New York, USA, 1955. January 2013.

[2] S. Din and A. Paul, "Smart health monitoring and management system: Toward autonomous wearable sensing for Internet of things using big data analytics", *Future Generation Computer Systems*, Elsevier, 2018.

[3] J. Loo, J. Mauri and J. Ortiz. "Mobile ad hoc networks: current status and future trends". London: CRC Press, 2016. ISBN 978-1-4200-8812-0.

[4] U. Jha and R. Prasad. "OFDM towards fixed and mobile broadband wireless access". London: Artech House, 2007. ISBN 978-1-58053-641-7.

[5] G. Tsoulos, "MIMO system technology for wireless communications", London: CRC press, 2006. ISBN 978-0849341908

[6] V. Tarokh, A. Naguib, N. Seshadri and A. R. Calderbank, "Space-time codes for high data rate wireless communication: performance criteria in the presence of channel estimation errors, mobility, and multiple paths," *IEEE Transactions on Communications*. 1999, vol. 47, pp. 199–207. ISSN 0090-6778.

[7] T. Schmidl and D. Cox. "Robust frequency and timing synchronization for OFDM", *IEEE Transactions on Communications*. 1997, vol. 45, pp. 1613–1621. ISSN 1558-0857.

[8] C. Jieping, "An improved training sequence based timing synchronization algorithm for MIMO-OFDM system", *Fifth International Conference on Intelligent Systems Design and Engineering Applications* . Hunan, China: IEEE, 2014.

[9] A. Sreedhar, S. Sekhar and S. Pillai, "An efficient preamble design for timing synchronization in MIMO-OFDM systems", *International Conference on Control, Instrumentation, Communication and Computational Technologies (ICCICCT)*. Kumaracoil, India: IEEE, 2015.

[10] L. Nasraoui, L. Atallah and M. Siala, "Robust Synchronization Approach for MIMO-OFDM Systems with Space-Time Diversity", *81st Vehicular Technology Conference (VTC Spring)*. Glasgow, UK: IEEE, 2015.

[11] A. Beydoun, H. Alaeddine and H. Elmokdad, "New fast time synchronization method for MIMO-OFDM systems", *11th IFIP Wireless and Mobile Networking Conference (WMNC)*. Prague: IEEE, 2018.

[12] A. Beydoun, and H. Alaeddine, "Low-complexity channel estimation algorithm for MIMO-OFDM systems", *World Academy of Science Engineering and Technology (WASET): International Journal of Computer and Systems Engineering* . 2019, vol. 3, eISSN:1307-6892.

[13] E. Larsson and P. Stoica, "Space-time block coding for wireless communications", London: Cambridge university press, 2008. ISBN 978-0511550065

[14] A. Shokair, A. Beydoun, D.G. Pham, C. Jabbour and P. Desgreys. "Wide band digital predistortion using iterative feedback decomposition". *Analog Integrated Circuits and Signal Processing*. 2018, vol. 0, pp. 1–16. ISSN 1573-1979.

[15] NI USRP 2920 Specifications. Available at: http://www.ni.com.

Ali Beydoun was born in Beirut, Lebanon, in 1980. He received a B.S. in Electronics from the Lebanese University in 2002, an Engineering Degree in Telecommunications from the ENSIETA school, Brest, France, in 2004 and a Ph.D in Electronics from Paris XI university in 2007. From 2007 to 2009, he was a research assistant at the Institut Telecom - ParisTech. Since October 2009, he is professor at the Lebanese university. His research interests include sigma delta modulation, acoustic echo cancellation, timing synchronization and channel estimation for MIMO OFDM system and digital processing for power amplifier linearization.

Hamzé H. Alaeddine was born in Lebanon, in1980. He received the B.Sc. degree in electronics from the Lebanese University, Lebanon, in 2002, and the M.Sc. degree from University of Brest, France, in 2003. In 2007, he received the Ph.D. degree from University of Brest, France. From 2008 to 2009, he was a Research Scientist with Department of Electrical Engineering, Ecole Polytechnique de Montréal, Canada. He joined in 2010 the Lebanese University. His research interests include Signal Processing for Telecommunications, adaptive filtering, echo cancellation, number theoretic transform and RF design for wireless systems.